Chemical Proteomic Analysis Reveals Alternative Modes of Action for Pyrido[2,3-*d*]pyrimidine Kinase Inhibitors*

Josef Wissing, Klaus Godl, Dirk Brehmer, Stephanie Blencke, Martina Weber, Peter Habenberger, Matthias Stein-Gerlach, Andrea Missio, Matt Cotten, Stefan Müller, and Henrik Daub‡

Small molecule inhibitors belonging to the pyrido[2,3-*d*]pyrimidine class of compounds were developed as antagonists of protein tyrosine kinases implicated in cancer progression. Derivatives from this compound class are effective against most of the imatinib mesylate-resistant *BCR-ABL* mutants isolated from advanced chronic myeloid leukemia patients. Here, we established an efficient proteomics method employing an immobilized pyrido[2,3-*d*]pyrimidine ligand as an affinity probe and identified more than 30 human protein kinases affected by this class of compounds. Remarkably, *in vitro* kinase assays revealed that the serine/threonine kinases Rip-like interacting caspase-like apoptosis-regulatory protein kinase (RICK) and p38α were among the most potently inhibited kinase targets. Thus, pyrido[2,3-*d*]pyrimidines did not discriminate between tyrosine and serine/threonine kinases. Instead, we found that these inhibitors are quite selective for protein kinases possessing a conserved small amino acid residue such as threonine at a critical site of the ATP binding pocket. We further demonstrated inhibition of both p38 and RICK kinase activities in intact cells upon pyrido[2,3-*d*]pyrimidine inhibitor treatment. Moreover, the established functions of these two kinases as signal transducers of inflammatory responses could be correlated with a potent *in vivo* inhibition of cytokine production by a pyrido[2,3-*d*]pyrimidine compound. Thus, our data demonstrate the utility of proteomic methods employing immobilized kinase inhibitors for identifying new targets linked to previously unrecognized therapeutic applications. ***Molecular & Cellular Proteomics 3: 1181–1193, 2004.***

Protein kinases are key control elements of cellular signaling, which is de-regulated in various diseases such as human cancer. Therefore, the protein kinase family of enzymes has emerged as a major class of drug targets in recent years (1). Pharmacological inhibition of protein kinases can be achieved with small molecule inhibitors, which block the catalytic activity of kinases by interfering with ATP binding. Various protein kinase-selective drugs are currently in different stages of clinical development and might enter the market in the near future. The phenylaminopyrimidine compound imatinib mesylate (Gleevec, STI571) was the first tyrosine kinase inhibitor receiving FDA approval, and this drug is successfully used for the treatment of chronic myeloid leukemia (CML)[1] (2). Imatinib, a potent inhibitor of the constitutive Bcr-Abl tyrosine kinase activity causative for CML pathogenesis, is highly effective in early phases of the disease, whereas resistance formation and subsequent therapy failure was observed in patients with advanced CML. Biochemical analysis of Bcr-Abl from relapsed patients revealed amino acid substitutions within the Abl kinase domain as a major cause of molecular resistance to imatinib (3–5). In addition to imatinib, inhibitors from the pyrido[2,3-*d*]pyrimidine class of compounds have been identified as highly effective Abl kinase blockers (6). Pyrido[2,3-*d*]pyrimidines were initially developed as broadly active inhibitors of several tyrosine kinases such as Src, platelet-derived growth factor receptor and fibroblast growth factor receptor (FGFR) (7, 8). In subsequent studies, derivatives out of this class of compounds were also shown to potently inhibit Bcr-Abl and c-kit tyrosine kinase activities (6, 9). Recently, pyrido[2,3-*d*]pyrimidine inhibitors of Abl activity were tested against various imatinib-resistant *BCR-ABL* isoforms detected in relapsed patients (10). The Thr-315 to isoleucine

From Axxima Pharmaceuticals AG, 81377 München, Germany
Received, September 8, 2004, and in revised form, October 7, 2004
Published, MCP Papers in Press, October 8, 2004, DOI 10.1074/mcp.M400124-MCP200

[1] The abbreviations used are: CML, chronic myeloid leukemia; 16-BAC, 16-benzyldimethyl-*n*-hexadecylammonium chloride; ATF2, activating transcription factor 2; CSK, C-terminal Src kinase; DMF, dimethylformamide; EDC, *N*-ethyl-*N*′-(3-dimethylaminopropyl) carbodiimide hydrochloride; EGF, epidermal growth factor; ERK, extracellular signal-regulated protein kinase; FAK, focal adhesion kinase; FBS, fetal bovine serum; FGFR, fibroblast growth factor receptor; GAK, cyclin G-associated kinase; HFF, human foreskin fibroblast; IFN-β, interferon-β; JNK, c-jun N-terminal kinase; LPS, lipopolysaccharide; MAPK, mitogen-activated protein kinase; MAPKAP-K2, MAPK-activated protein kinase 2; MBP, myelin basic protein; MEK1, MAPK/ERK kinase 1; MIP-1α, macrophage inflammatory protein-1α; MS, mass spectrometry; PBMC, peripheral blood mononuclear cell; PP58, pyrido[2,3-*d*]pyrimidine derivative 58; RICK, Rip-like interacting caspase-like apoptosis-regulatory protein kinase; Rsk1, ribosomal S6 protein kinase 1; SRPK1, SR protein-specific kinase 1; TNF-α, tumor necrosis factor-α.

substitution, which directly interferes with inhibitor binding at the ATP-binding pocket, rendered Bcr-Abl resistant to both imatinib and the pyrido[2,3-*d*]pyrimidine PD180970 (Fig. 1). But, remarkably, all other clinically relevant Bcr-Abl variants tested by La Rosée *et al.* had retained their sensitivity to inhibition by PD180970. These included the Y253F, E255K, and M351T mutants frequently detected in imatinib-insensitive patients, which either interfere with the distorted conformation of the ATP-binding loop or the closed conformation of the activation loop critical for imatinib binding (3–5, 11, 12). Thus, pyrido[2,3-*d*]pyrimidine-based drugs could show efficacy in many cases of imatinib-resistant CML, because constitutive Bcr-Abl activity remains causative for further disease progression. Previous *in vivo* testing of pyrido[2,3-*d*]pyrimidine kinase inhibitors has demonstrated inhibition of tumor growth, but, due to the limited solubility of these compounds, no consistent dose-dependent effect could be observed in mouse xenografts (8, 13, 14). Thus, additional efforts in medicinal chemistry are obviously needed to confer better drug-like properties to this class of compounds. Moreover, in accordance with nonspecific toxic effects previously attributed to pyrido[2,3-*d*]pyrimidine kinase inhibitors, selectivity remains a critical issue that has to be evaluated for derivatives of this versatile compound scaffold (9).

Inhibitor selectivity is usually examined against panels of protein kinases, in which the activities of various recombinant enzymes are tested for their sensitivities to an inhibitor (15, 16). Although this established strategy provides useful results about the relative selectivity of an inhibitor, it has several shortcomings because only a small subset of the more than 500 human protein kinases can be tested and alternative protein targets such as different types of enzymes are usually excluded altogether (17). A conceptually different approach to study inhibitor function employs suitable small molecule derivatives, which can be covalently immobilized on chromatography beads and then used for the affinity purification of cellular target proteins (18–21). In combination with sensitive MS analysis, this chemical proteomics strategy has the potential to reveal the cellular target proteins of small molecule inhibitors in extracts from cultured cells, tissues, or even whole organisms. The successful implementation of chemical proteomic techniques critically depends on the efficiency and performance of the affinity purification procedures. We have recently reported an affinity chromatography technique, which operates under optimized biochemical conditions and allowed the identification of several previously unknown cellular targets of the p38 inhibitor SB 203580 and bisindolylmaleimide-type protein kinase C inhibitors (22–24).

Here, we have adapted this proteomic approach for a pyrido[2,3-*d*]pyrimidine derivative and identified more than 30 new cellular protein kinase targets of this inhibitor class. Remarkably, both the *in vitro* and cellular activities of the identified serine/threonine kinases Rip-like interacting caspase-like apoptosis-regulatory protein kinase (RICK) and p38α were potently blocked by the pyrido[2,3-*d*]pyrimidine inhibitor used in this study. In agreement with their established roles during inflammatory cytokine biosynthesis, pyrido[2,3-*d*]pyrimidine inhibitor treatment interfered with various innate immune responses such as the lipopolysaccharide (LPS)-induced tumor necrosis factor-α (TNF-α) release from monocytic cells. Thus, we demonstrate the utility of a protein kinase inhibitor-based proteomics strategy for the identification of novel targets linked to previously unrecognized therapeutic applications.

EXPERIMENTAL PROCEDURES

Reagents and Plasmids—Cell culture media and LipofectAMINE were obtained from Invitrogen (San Diego, CA). Radiochemicals, ECH Sepharose 4B, and poly(I:C) were purchased from Amersham Biosciences (Uppsala, Sweden). Histone was obtained from Roche (Basel, Switzerland). GST-activating transcription factor 2 (ATF2), GST-Crk, catalytically inactive GST-extracellular signal-regulated protein kinase 2 (ERK2), and kemptide were obtained from Upstate (Lake Placid, NY). All other reagents were obtained from Sigma (St. Louis, MO).

Antibodies used were mouse monoclonal anti-v-Src (Oncogene, San Diego, CA), mouse monoclonal anti-Abl (Pharmingen, San Diego, CA), rabbit polyclonal anti-RICK (Affinity BioReagents, Golden, CO), mouse monoclonal anti-cyclin G-associated kinase (GAK) (MoBiTec, Gottingen, Germany), mouse monoclonal anti-Yes, mouse monoclonal anti-SR protein-specific kinase 1 (SRPK1), and mouse monoclonal anti-Aurora A (all three from BD Transduction Laboratories, Lexington, KY). Antibodies purchased from Cell Signaling Technology (Beverly, MA) were rabbit polyclonal anti-p38, rabbit polyclonal anti-mitogen-activated protein kinase-activated protein kinase 2 (MAPKAP-K2), rabbit polyclonal anti-phospho-MAPKAP-K2 (Thr-344), rabbit polyclonal anti-phospho-ribosomal S6 protein kinase 1 (Rsk1) (Thr-359/Ser-363). Antibodies obtained from Santa Cruz Biotechnology (Santa Cruz, CA) were rabbit polyclonal anti-FGFR1, rabbit polyclonal anti-c-jun N-terminal kinase (JNK)1/2, rabbit polyclonal anti-ERK1/2, rabbit polyclonal anti-focal adhesion kinase (FAK), rabbit polyclonal anti-C-terminal Src kinase (CSK), rabbit polyclonal anti-MAPK/ERK kinase 1 (MEK1), rabbit polyclonal anti-Wee1, rabbit polyclonal anti-Rsk1, and mouse monoclonal anti-Lyn.

Recombinant protein kinases from commercial sources were human p38α, human JNK2α 2, human Aurora A, human MEK1, human EphB4, human Src (all from Upstate), and mouse Abl (New England Biolabs, Beverly, MA).

Site-directed mutagenesis of the previously described plasmid pGEX-4T1-GAK was performed according to the manufacturer's protocol (Stratagene, La Jolla, CA) (22). Recombinant wild-type and mutant GAK were expressed as GST fusion proteins in *Escherichia coli* as described (22). Recombinant RICK enzyme production using adenovirus-directed expression was performed as described (25). The RICK and FGFR1 plasmids for expression in mammalian cells have been described elsewhere (22, 26).

Compound Synthesis and Covalent Coupling—The pyrido[2,3-*d*]pyrimidine kinase inhibitors referred to as PP58 and PP58peg in this study were made by and purchased from Evotec-OAI. PP58 was synthesized as previously described (8). PP58peg was prepared by dissolving 0.44 mmol PP58, 0.44 mmol 1-bromo-2-[2-(2-ethoxy-ethoxy)-ethoxy]-ethane, and 0.44 mmol diisopropylamine in 10 ml of 1,4-dioxane and refluxing the reaction mixture for 36 h. The solution was cooled to room temperature, and the solvent was removed under vacuum. The residue was purified by column chromatography [silica gel; dichloromethane/methanol (95:5)] to yield PP58peg as a yellow solid.

For PP58 immobilization, 2.5 ml of drained ECH Sepharose 4B

were washed three times with 50 ml of 0.5 M NaCl, twice with 50 ml of H_2O and finally once with 50 ml of 50% dimethylformamide (DMF)/50% EtOH. Then 2.5 ml of drained beads were resuspended in 5 ml of a 0.75 mM solution of PP58 dissolved in 50% DMF/50% EtOH followed by the addition of 750 μl of 1 M *N*-ethyl-*N*′-(3-dimethylaminopropyl) carbodiimide hydrochloride (EDC) in 50% DMF/50% EtOH. After incubation overnight at room temperature with continual agitation in the dark, beads were washed three times with 15 ml of 50% DMF/50% EtOH prior to the addition of 5 ml of 33% DMF/33% EtOH/34% 1 M ethanolamine pH 8.0 and 650 μl of 1 M EDC. After 2-h incubation at room temperature with continual agitation in the dark, beads were washed three times with 15 ml of 50% DMF/50% EtOH, twice with 15 ml of 0.5 M NaCl and once with 15 ml of 20% EtOH. The obtained beads were stored in the dark at 4 °C as a suspension in 20% ethanol.

Cell Culture, Lysate Preparation, and in Vitro Association Experiments—COS-7, HeLa, U373, and human foreskin fibroblast (HFF) cells were maintained in Dulbecco's modified Eagle medium supplemented with 10% fetal bovine serum (FBS). COS-7 cell transfections, [^{32}P]orthophosphate labeling, and the analysis of cellular RICK kinase activity was performed as previously described (22, 27).

To examine the cellular p38 and ERK activities in the presence of different PP58 concentrations, HeLa cells were lysed with buffer containing 10 mM Tris-HCl pH 7.5, 150 mM NaCl, 1 mM EDTA, 1% Triton X-100, 1% sodium deoxycholate, 0.1% SDS plus additives (10 mM sodium fluoride, 1 mM orthovanadate, 10 μg/ml aprotinin, 10 μg/ml leupeptin, 1 mM PMSF, 1 mM DTT). After SDS-PAGE, immunoblotting with phospho-specific antisera detecting the phosphorylation of either the cellular p38 substrate MAPKAP-K2 or the cellular ERK substrate Rsk1 provided a read-out for cellular p38 and ERK activities.

For *in vitro* association with inhibitor affinity beads, HeLa cells or transfected COS-7 cells were lysed in buffer containing 50 mM HEPES pH 7.5, 150 mM NaCl, 0.5% Triton X-100, 1 mM EDTA, 1 mM EGTA plus additives. After centrifugation, lysates were adjusted to 1 M NaCl prior to *in vitro* association of 200 μl of high salt lysate with either 20 μl of drained PP58 matrix or control matrix for 3 h at 4 °C. Where indicated, 1 mM free PP58 was added to the lysate. After three washing steps with lysis buffer containing 1 M NaCl, the beads were eluted with 40 μl of 1.5× SDS sample buffer. After SDS-PAGE, proteins were transferred to nitrocellulose membrane and immunoblotted with the indicated antibodies.

Affinity Chromatography and Preparative Gel Electrophoresis—Frozen HeLa cells (2.5×10^9; Cilbiotech, Mons, Belgium) were lysed in 30 ml of the same Triton X-100-containing buffer plus additives used for sample preparation prior to the analytical *in vitro* association experiments. Affinity chromatography using PP58 columns was then performed essentially according to the previously described protocol for the purification of cellular targets of immobilized SB 203580-related inhibitor (22). After elution of bound proteins with buffer containing 1 mM PP58 and 10 mM ATP, a second elution step was performed using lysis buffer containing 0.5% SDS. Both elution fractions were concentrated and precipitated as described. Two-thirds of the first elution fraction were resolved by 16-benzyldimethyl-*n*-hexadecylammonium chloride (16-BAC)/SDS-PAGE, and the remaining material was used for LC-MS/MS analysis (22, 27).

Mass Spectrometry—Gel-excised protein spots and protein bands were trypsin-digested and then analyzed by MALDI mass mapping on a Bruker Ultraflex TOF/TOF mass spectrometer (Bruker, Billerica, MA) as described (22, 28). For nano-HPLC MS/MS, proteins eluted from PP58 columns were resolved by SDS-PAGE over a separation distance of only about 12 mm. After staining with Coomassie blue, the gel was cut into slices and the protein content in each fraction was estimated using the Pharmacia (Uppsala, Sweden) low molecular weight protein standard and BSA as the reference protein at a concentration of 1 μg per lane and AIDA software (raytest, Straubenhardt, Germany) for quantification. Protein digest and peptide isolation was carried out as for MALDI samples.

The separation of the peptide samples was performed using a bioinert Ultimate nano-HPLC system (Dionex, Sunnyvale, CA). Then 10 μl of each sample (containing up to 1 μg peptides) were injected, and peptides were purified and concentrated on a C_{18}-PepMap precolumn (0.3 mm inner diameter × 5 mm, 100 Å pore size, 3 μm particle size) at a flow rate of 30 μl/min in 0.1% TFA. Subsequently, peptides were separated on an analytical 75 μm inner diameter × 150 mm C_{18}-PepMap column (Dionex; 100 Å pore size, 3 μm particle size) at a column flow rate of 200 nl/min. The gradient (Solution A: 0.1% formic acid, 5% ACN; solution B: 0.1% formic acid, 80% ACN) started at 5% and ended at 60% B after 90 min.

MS and MS/MS data were acquired using a Q-TOF II mass spectrometer (Waters Corp., Micromass, Manchester, United Kingdom). Doubly and triply charged peptide-ions were automatically chosen by the MassLynx software and fragmented for a maximum of 18 s for each peptide. MS data were automatically processed and peaklists for protein identifications by database searches were generated by the MassLynx software. Database searches were carried out with an in-house MASCOT server using the NCBI protein database.

In Vitro Kinase Assays—Substrate phosphorylation reactions were linear with respect to time in all kinase activity assays and therefore represented the initial velocities. Kinase assays of p38α, RICK, GAK, and JNK2 were performed as described in the presence of the indicated PP58 concentrations and 50 μM cold ATP (22). For K_i determination, p38α was also assayed at 100, 150, and 200 μM ATP, and JNK2 was also tested at 5, 10, and 25 μM ATP. PP58 inhibition of Abl, Src, and EphB4 activities were assayed for 30 min at 30 °C in a reaction buffer containing 20 mM Tris-HCl pH 7.5, 10 mM $MgCl_2$, 0.8 mM $MnCl_2$, 1 mM DTT, 0.1 mM EGTA, 100 μM sodium orthovanadate, 50 μM ATP, 2 μCi [γ-^{32}P]ATP, and 0.2 mg/ml GST-Crk, 0.4 mg/ml myelin basic protein (MBP), or 0.2 mg/ml glyceraldehyde-3-phosphate dehydrogenase as kinase substrates, respectively.

MEK1 and Aurora A activities were tested at 37 °C in a total volume of 30 μl. The kinases were assayed according to the manufacturer's protocol using 50 μM ATP and 1 μCi [γ-^{32}P]ATP in the presence of different PP58 concentrations. Kinase substrate proteins included were 0.25 mg/ml inactive GST-ERK2 for MEK1 and 0.025 mg/ml kemptide for Aurora A, respectively. Reactions, in which protein substrates were used to measure kinase activities, were stopped by addition of SDS sample buffer. After gel electrophoresis, phosphorylated substrate proteins were visualized by autoradiography and quantified by phosphoimaging. For quantification of Aurora A kinase-mediated peptide substrate phosphorylation, peptides were bound to Whatman P51 paper, washed, and ^{32}P incorporation was then measured in a scintillation counter. Determination of IC_{50} [0–100%] values was performed using GraFit software (Erithacus, Horley, Surrey, United Kingdom).

Cytokine Assays—Frozen human peripheral blood mononuclear cells (PBMCs) were purchased from Cambrex Bio Science (East Rutherford, NJ). Thawed and washed cells were resuspended in RPMI 1640 medium containing 1% FBS and then seeded into 24 well dishes (1×10^6 cells per well). After 1 h, the medium was aspirated, the cell culture plates were washed with medium to remove nonadherent cells and fresh medium was added. The medium was exchanged again after a further 3.5 h prior to addition of either Me_2SO or different amounts of PP58 and subsequent LPS (Sigma; serotype 055:B5) stimulation of the human PBMCs. Sixteen hours later, supernatants were harvested and analyzed using ELISA kits from R&D Systems to quantify the levels of TNF-α, macrophage inflammatory protein-1α (MIP-1α), and IL-8 released into the medium. Prior to

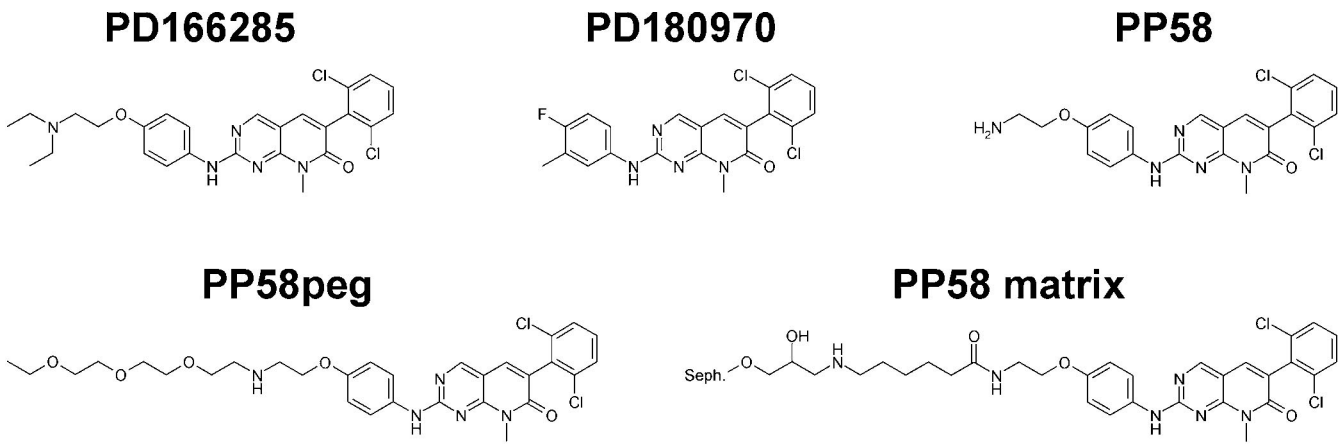

FIG. 1. **Chemical structures of pyrido[2,3-*d*]pyrimidine-based compounds and the inhibitor affinity matrix.** The pyrido[2,3-*d*]pyrimidine PP58 is related in structure to PD166285 and PD180970. Pegylation of PP58 yielded PP58peg. Carbodiimide coupling resulted in covalent immobilization of PP58 on ECH Sepharose 4B.

inhibitor and subsequent LPS or poly(I:C) treatment, confluent HFF cells were incubated with fresh DMEM containing 1% FBS for 30 min. After 16 h of ligand stimulation, IL-8 levels in the supernatants were measured. All cytokine assays were performed according to the manufacturer's instructions.

U373 cell stimulations were also performed in DMEM/1% FBS, and total RNA was isolated 2 h after poly(I:C) treatment using the Trizol method (Invitrogen) followed by a DNase I digest on RNeasy columns (Qiagen, Hilden, Germany). Interferon-β (IFN-β) mRNA levels were determined by quantitative RT-PCR based on the 5′ exonuclease activity of Taq polymerase on an ABI PRISM 7000 Sequence Detection System (Applied Biosystems, Foster City, CA). RNA was reverse transcribed with Superscript II (Invitrogen) and oligo-dT primers according to the manufacturer's protocol. Gene-specific TaqMan probes were labeled with FAM™ at the 5′ end and TAMRA™ at the 3′ end of the oligonucleotides. Glyceraldehyde-3-phosphate dehydrogenase (determined with pre-developed TaqMan assay reagents from Applied Biosystems) served as a housekeeping gene. Primer sequences for IFN-β were: 5′-GACATCCCTGAGGAGATTAAGCA-3′ (forward), reverse: 5′-GGAGCATCTCATAGATGGTCAATG-3′ (reverse), 5′-FAM-CGTCCTCCTTCTGGAACTGCTGCAG-TAMRA-3′ (TaqMan probe).

RESULTS

Generation of a Functional Pyrido[2,3-d]pyrimidine Inhibitor Affinity Matrix—Derivatives from the pyrido[2,3-*d*]pyrimidine class of compounds were originally identified as potent inhibitors of several protein tyrosine kinases such as the FGFR1 and Src (8). PD166285, one of the most potent and soluble analogues of this initial series (Fig. 1), was characterized in a variety of cellular assays and later found to block Wee1 kinase activity at nanomolar concentrations (7, 29). The search for alternative inhibitors of cellular Bcr-Abl activity led to the identification of pyrido[2,3-*d*]pyrimidine derivatives such as PD180970, which potently interfered with the tyrosine kinase activities of Abl and c-kit in the low nanomolar range (Fig. 1) (6, 9). The crystal structure of the Abl kinase domain in complex with a similar pyrido[2,3-*d*]pyrimidine compound demonstrated exposure of the inhibitors 2-anilino substituent at the protein surface (30). Based on these structural data, we reasoned that a previously described analogue exposes a primary amino function into the solvent and should therefore retain its protein kinase binding properties after covalent immobilization at this substituent. This inhibitor is shown in Fig. 1 and has been described as derivative 58 out of a series of pyrido[2,3-*d*]pyrimidines (8). We therefore refer to this compound as PP58 in this study. PP58 was then pegylated at the primary amino position. The resulting compound PP58peg "topologically" mimics immobilized PP58, which was obtained by covalent coupling to the free carboxyl groups of ECH Sepharose in the presence of carbodiimide (Fig. 1). Both PP58 and PP58peg were then tested in *in vitro* assays of Src kinase activity using MBP as a substrate protein (31). Importantly, pegylation of PP58 did not have a significant effect on the inhibitor's potency to suppress Src kinase activity (Fig. 2*A*). Thus, extension of PP58 at its primary amine did not interfere with kinase binding, a result that identified this moiety as ideal site for covalent immobilization of the inhibitor. Notably, PP58 inhibited Src with a subnanomolar IC_{50} value in our assays, which is more than an order of magnitude below the IC_{50} value of 13 nM reported earlier (8). This discrepancy is most likely due to the much lower Src enzyme concentrations present in our assays. In our experiments, we observed that PP58 behaved as a titration reagent at higher Src protein concentrations. To measure Src activities at low enzyme concentrations, it was also necessary to analyze the phosphorylation of a protein substrate, which could be quantified after gel electrophoretic separation. This experimental design features a more favorable ratio of measureable kinase activity to background signal compared with filter binding assays of kinase substrate phosphorylation.

To test whether endogenously expressed Src kinase specifically interacts with the pyrido[2,3-*d*]pyrimidine affinity matrix, we subjected total cell lysates from HeLa cells to *in vitro* association with either control beads or PP58 beads in the absence or presence of free PP58 compound. As analyzed by

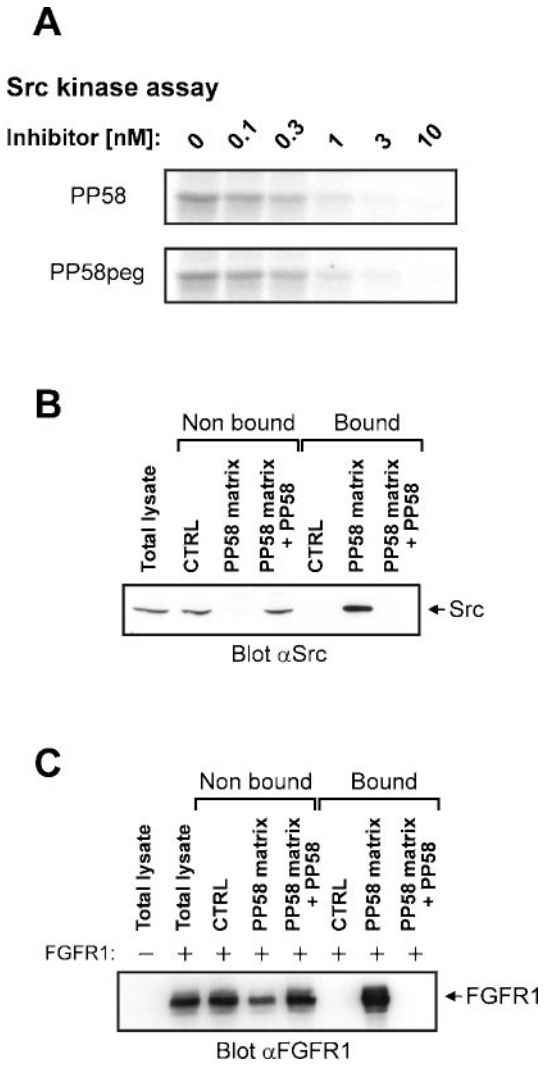

FIG. 2. **Characterization of pegylated and immobilized PP58.** *A*, *in vitro* phosphorylation of MBP by recombinant Src tyrosine kinase was performed in the presence of the indicated concentrations of PP58 and PP58peg. After SDS-PAGE, ^{32}P incorporation into MBP was visualized by autoradiography. *B*, total lysate from HeLa cells was used for *in vitro* association with either control beads (CTRL) or the PP58 affinity matrix. Free PP58 was added to the lysate where indicated. Total lysate, the supernatant fractions and the bound proteins eluted from control or PP58 beads were resolved by SDS-PAGE and analyzed by immunoblotting with Src-specific antibody. Relative to the total cell lysate and the supernatants, 10× aliquots of bound protein fractions were loaded on the gel. *C*, total cell extracts from either control- or FGFR1-transfected COS-7 cells were prepared. Lysate from FGFR1-expressing cells was subjected to *in vitro* association and SDS-PAGE as described above. Immunoblotting was then performed with FGFR1-specific antiserum. FGFR1 expression was not detectable in control-transfected COS-7 cells.

immunoblotting with specific antiserum, the PP58 matrix specifically depleted Src from total lysate, whereas binding to the PP58 beads was prevented when free inhibitor was included (Fig. 2*B*). To verify the functionality of the pyrido[2,3-*d*]pyrimidine matrix with a second known inhibitor target, we prepared total cell lysate from FGFR1-expressing COS-7 cells for *in vitro* binding studies. As shown in Fig. 2*C*, the ectopically expressed FGFR1 receptor tyrosine kinase was specifically retained on PP58 beads. In conclusion, these experiments established the PP58 matrix as a novel affinity reagent for the purification of cellular pyrido[2,3-*d*]pyrimidine inhibitor targets.

Purification of Cellular Pyrido[2,3-d]pyrimidine Inhibitor Targets by Affinity Chromatography—To characterize the cellular targets of the pyrido[2,3-*d*]pyrimidine inhibitor PP58 on a proteome-wide scale, we loaded total cell extract from 2.5×10^9 HeLa cells on a PP58 affinity column using a protocol adapted from our previously described procedures (22, 23). After extensive washing, bound proteins were specifically released from the inhibitor column with running buffer containing free PP58 and ATP. Eluted proteins were then precipitated and two-thirds of the purified material were resolved by preparative 16-BAC/SDS-PAGE. Subsequent Coomassie staining allowed the detection of more than 50 protein spots (Fig. 3*A*), which were cut out from the gel and analyzed by mass fingerprinting using a MALDI-TOF/TOF mass spectrometer. Selected peptides were further characterized by PSD fragmentation. Strikingly, the majority of the excised spots contained protein kinases and almost 25 different members of this enzyme class could be identified from the preparative 16-BAC/SDS gel (Fig. 3*A*). A list of the characterized protein spots is shown in Table I. Among the identified cellular targets were several cytoplasmatic tyrosine kinases such as FAK, TEC, JAK1, Fer, the Src-related kinase Yes, and, represented by one of the most prominent spots, CSK, which negatively regulates Src family enzymes through phosphorylation of a conserved C-terminal tyrosine residue (32). Although Src itself specifically bound to the PP58 matrix as shown above, it was not identified from the gel. Most likely, Src co-migrates with its more abundant relative Yes and is therefore covered by the rather prominent Yes protein spot. Interestingly, Abl tyrosine kinase, a known pyrido[2,3-*d*]pyrimidine inhibitor target, could be identified in the high molecular weight region of the gel. In addition to cytoplasmatic tyrosine kinases, the MS data also revealed the receptor tyrosine kinases EphB2, EphB4, and Ron as pyrido[2,3-*d*]pyrimidine-interacting proteins. Taken together, these identifications of various new tyrosine kinase targets of pyrido[2,3-*d*]pyrimidines support the concept that derivatives from this compound class are rather broadly active tyrosine kinase inhibitors.

Surprisingly, the perhaps most prominent protein spot on the gel was not a tyrosine kinase but instead represented the Ser/Thr protein kinase p38α (Fig. 3*A*). In addition to p38α, we identified several other Ser/Thr kinases involved in mitogen-activated protein kinase (MAPK) signaling. Furthermore, MS revealed RICK (also known as Rip2 or CARDIAK), GAK and PKN3 as cellular targets. These Ser/Thr kinases were also identified in an earlier study, in which we used the same proteomic strategy to characterize the cellular targets of the p38 inhibitor SB 203580. From these results, it appears that

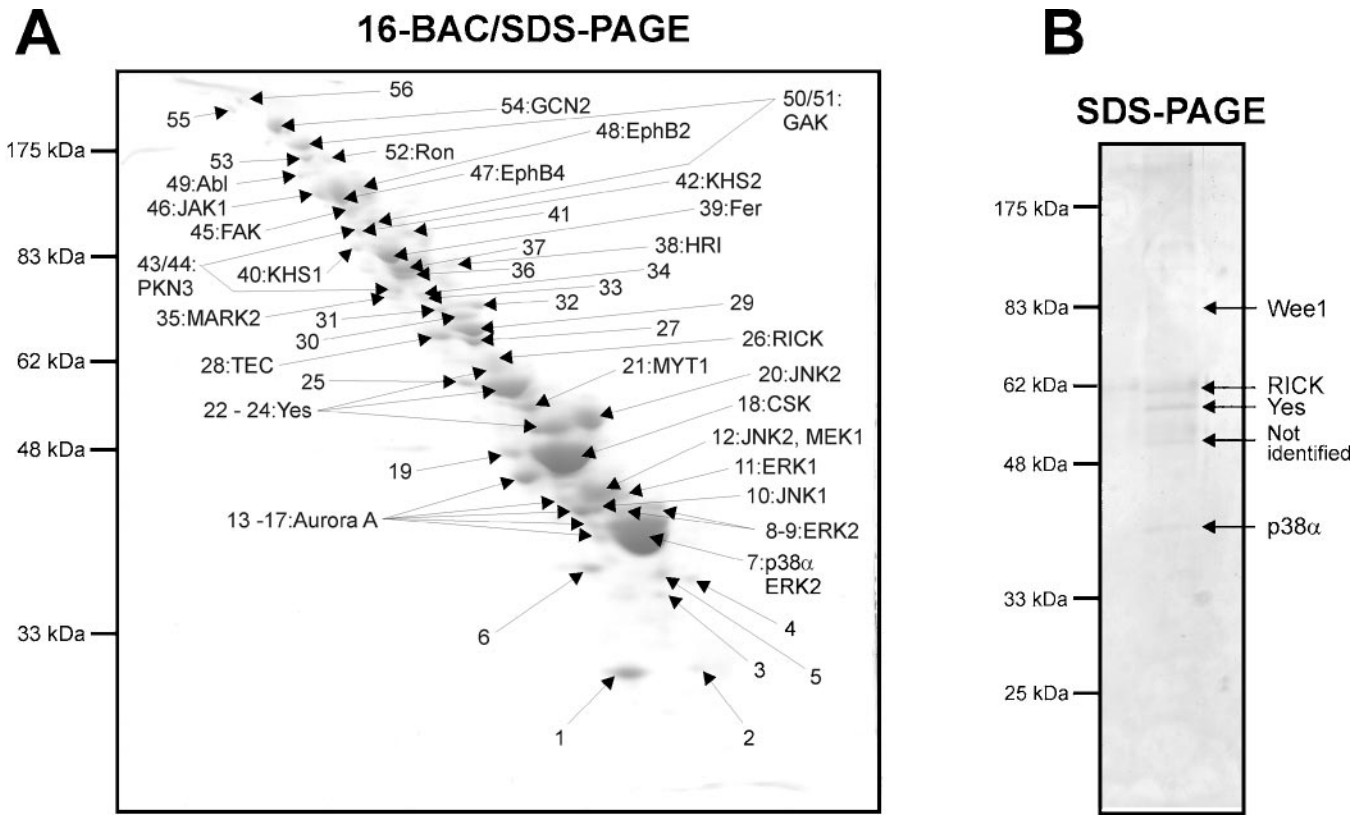

FIG. 3. **Affinity purification of cellular pyrido[2,3-*d*]pyrimidine inhibitor targets.** HeLa cell extract was prepared and loaded onto a PP58 column. Specifically bound proteins were first eluted with buffer containing both free PP58 and ATP. *A*, two-thirds of the elution fraction were resolved by 16-BAC/SDS-PAGE, stained with Coomassie blue, and the visualized protein spots were then analyzed by MS. Identified proteins are listed in Table I. The remainder of the eluted proteins were used for LC-MS/MS analysis. Results are shown in Table II. *B*, after the first elution step, remaining bound proteins were released from the PP58 affinity column with SDS-containing buffer and separated by SDS-PAGE. Coomassie-stained protein bands were subjected to MS analysis.

pyrido[2,3-*d*]pyrimidine and pyridinyl imidazole inhibitors have an overlapping set of cellular protein kinase targets. Most of the other analyzed protein spots represented abundant cellular protein species not belonging to the superfamily of protein kinases. Although several of these identified proteins also bind nucleotides such as ATP or NADH and could therefore be potential PP58 targets, their presence in the elution fraction was most likely due to their high cellular abundance that compensated for a rather weak affinity of these proteins for the PP58 matrix (Fig. 3*A*, Table I). To test this assumption for one of the nonprotein kinase targets, we analyzed the activity of lactate dehydrogenase *in vitro* and did not detect any significant inhibitory effect of 100 μM PP58 on this enzyme (data not shown).

In addition, we performed nanoflow reversed-phase HPLC-MS/MS analysis using a Q-TOF mass spectrometer. For this purpose, smaller aliquots of the cellular target protein fraction purified by PP58 affinity chromatography were resolved over a short distance in a SDS gel. After incubation of gel slices with trypsin, the eluted peptides were subjected to LC-MS/MS analysis. This approach revealed 10 additional cellular protein kinase targets of the pyrido[2,3-*d*]pyrimidine PP58 such as the tyrosine kinases Fyn, Lyn, BLK, DDR2, and EphA2. Protein kinase identifications from these experiments are shown in Table II. Interestingly, PP58 affinity chromatography led to the identification of protein kinases belonging to various different groups and families, indicating that the pyrido[2,3-*d*]pyrimidine inhibitor is not selective for a set of phylogenetically related members of the human kinome (Tables I and II). Moreover, several kinases found in the 16-BAC/SDS gel were not detected by LC-MS/MS and vice versa. Thus, even when highly enriched subfractions of the proteome are analyzed as in our study, these two different proteomic approaches delivered complementary sets of results. This observation is in accordance with various studies in which both two-dimensional gel-MS and LC-MS/MS identification strategies have been applied to more complex protein mixtures such as total cell extracts (33, 34).

Finally, we performed a second elution step using SDS-containing buffer to release any remaining bound proteins from the PP58 affinity column. Subsequent SDS-PAGE revealed a few Coomassie-stainable protein bands and the protein kinases Yes, RICK, Wee1, and p38α could be identified by MS (Fig. 3*B*). With the exception of Wee1, all of these

TABLE I
Results from MS analysis of proteins isolated after 16-BAC/SDS-PAGE

Spot no.	Protein name	Gi no.[a]	M_r [Da]	Group/family[b]
1	Methylthioadenosine phosphorylase	4505273	31,250	–
2	Not identified	–	–	–
3	HSP27	662841	22,327	–
4	Lactate dehydrogenase	13786847	36,507	–
4	Protein phosphatase 4	4506027	35,080	–
5	Pyridoxal kinase	13543317	31,808	–
6	Glyceraldehyde-3-phosphate dehydrogenase	31645	36,054	–
7	p38 α	4503069	41,493	CMGC/MAPK
7	ERK2	20986531	41,390	CMGC/MAPK
8	ERK2	20986531	41,390	CMGC/MAPK
9	ERK2	20986531	41,390	CMGC/MAPK
10	JNK1	20986519	44,022	CMGC/MAPK
11	ERK1	186696	42,106	CMGC/MAPK
12	JNK2	1463129	44,024	CMGC/MAPK
12	MEK1	5579478	43,439	STE/STE7
13	Aurora A	27923855	45,809	Other/AUR
14	Aurora A	27923855	45,809	Other/AUR
15	Aurora A	27923855	45,809	Other/AUR
16	Aurora A	27923855	45,809	Other/AUR
17	Aurora A	27923855	45,809	Other/AUR
18	CSK	4758078	50,704	TK/Csk
19	Eukaryotic translation elongation factor 1α	4503471	50,140	–
20	JNK2	1463129	44,029	CMGC/MAPK
21	MYT1	2914671	53,992	Other/WEE
22	Yes	4885661	60,801	TK/Src
23	Yes	4885661	60,801	TK/Src
24	Yes	4885661	60,801	TK/Src
25	Pyruvate kinase 3	33286418	57,937	–
26	RICK	4506537	61,195	TKL/RIPK
27	Not identified	–	–	–
28	TEC	4507429	73,629	TK/Tec
29	Heat shock 70-kDa protein 8	5729877	70,898	–
30	Heat shock 70-kDa protein 9B	24234688	73,680	–
31	Moesin	14625824	61,872	–
32	Heat shock 70-kDa protein 5	16507237	72,333	–
33	Radixin	4506467	68,564	–
34	Ezrin	21614499	69,413	–
35	MARK2	9845487	83,205	CAMK/CAMKL
36	Heat shock 90-kDa protein 1β	20149594	83,264	–
37	Heat shock 90-kDa protein 1β	20149594	83,264	–
38	HRI	7839458	71,315	Other/PEK
39	Fer	4885231	94,624	TK/Fer
40	KHS1	30316147	95,040	STE/STE20
42	Heat shock protein gp96	15010550	90,194	–
42	KHS2	25987447	98,954	STE/STE20
43	PKN3	40254851	99,421	AGC/PKN
44	PKN3	40254851	99,421	AGC/PKN
45	FAK	24476013	119,233	TK/Fak
46	JAK1	4504803	131,957	TK/JakA
47	EphB4	16209618	108,270	TK/Eph
48	EphB2	17975765	117,493	TK/Eph
49	Abl	514268	124,955	TK/Abl
50	GAK	4885251	143,165	Other/NAK
51	GAK	4885251	143,165	Other/NAK
52	Ron	4505265	152,227	TK/Met
53	Carbamoylphosphate synthetase 1	21361331	164,939	–
54	GCN2	7243057	169,235	Other/PEK
55	Not identified	–	–	–
56	Not identified	–	–	–

[a] NCBI GenBank™ accession number.
[b] Classification of the identified protein kinases into groups and families according to Manning *et al.* (17).

TABLE II
Protein kinase targets identified by LC-MS/MS

Protein name	Gi no.[a]	M_r [Da]	Group/family[b]
Abl	514268	124,955	TK/Abl
Arg	6382062	128,343	TK/Abl
BLK	914204	57,757	TK/Src
CSK	4758078	50,704	TK/Csk
DDR2	5453814	96,752	TK/DDR
EphA2	125333	108,254	TK/Eph
EphB2	12644190	117,507	TK/Eph
EphB4	16209618	108,270	TK/Eph
ERK1	232066	43,136	CMGC/MAPK
ERK2	23879	40,420	CMGC/MAPK
Fer	4885231	94,624	TK/Fer
Fyn	4503823	60,762	TK/Src
GAK	4885251	143,165	Other/NAK
JNK1	20986519	44,022	CMGC/MAPK
JNK2	1082266	48,149	CMGC/MAPK
Lyn	187271	56,033	TK/Src
MEK1	5579478	43,439	STE/STE7
MEK2	13489054	44,424	STE/STE7
MYT1	2914671	53,992	Other/WEE
NEK2	31807297	37,956	Other/NEK
p38α	2499600	41,293	CMGC/MAPK
p38β	20128774	41,357	CMGC/MAPK
RICK	4506537	61,195	TKL/RIPK
Yes	4885661	60,801	TK/Src
ZAK	7542537	91,264	TKL/MLK

[a] NCBI GenBank™ accession number.
[b] Classification of the identified protein kinases into groups and families according to Manning *et al.* (17).

kinases were also detected in protein spots from the preparative 16-BAC/SDS gel, but were not quantitatively released from the column by the combined use of free PP58 and ATP as elution reagents. This might indicate a particular high affinity of these targets to the immobilized inhibitor.

In Vitro Characterization of Pyrido[2,3-d]pyrimidine Inhibitor Targets—To verify the MS results with a secondary assay, total cell extracts from HeLa cells were used for *in vitro* association studies with either control matrix or PP58 matrix with or without free pyrido[2,3-*d*]pyrimidine compound added to the incubations. Total cell lysate, nonbound proteins from the supernatant fractions and proteins retained by the affinity beads were then resolved by gel electrophoresis and subjected to immunoblotting with specific antibodies against protein kinases identified by MS (Fig. 4). All of the analyzed kinases could be confirmed as specific binders of the PP58 matrix. As a negative control, we probed for the Ser/Thr kinase SRPK1, which is expressed in HeLa cells and did not interact with the PP58 affinity material (Fig. 4).

Although the different PP58 kinase targets were more or less quantitatively depleted from the lysate by the inhibitor beads, this type of assay does not yield quantitative data about their respective sensitivities to PP58. To address this important issue, we performed *in vitro* kinase assays for the three tyrosine kinases Src, Abl, and EphB4 and the six Ser/Thr kinases p38α, RICK, GAK, MEK1, JNK2, and Aurora A in the

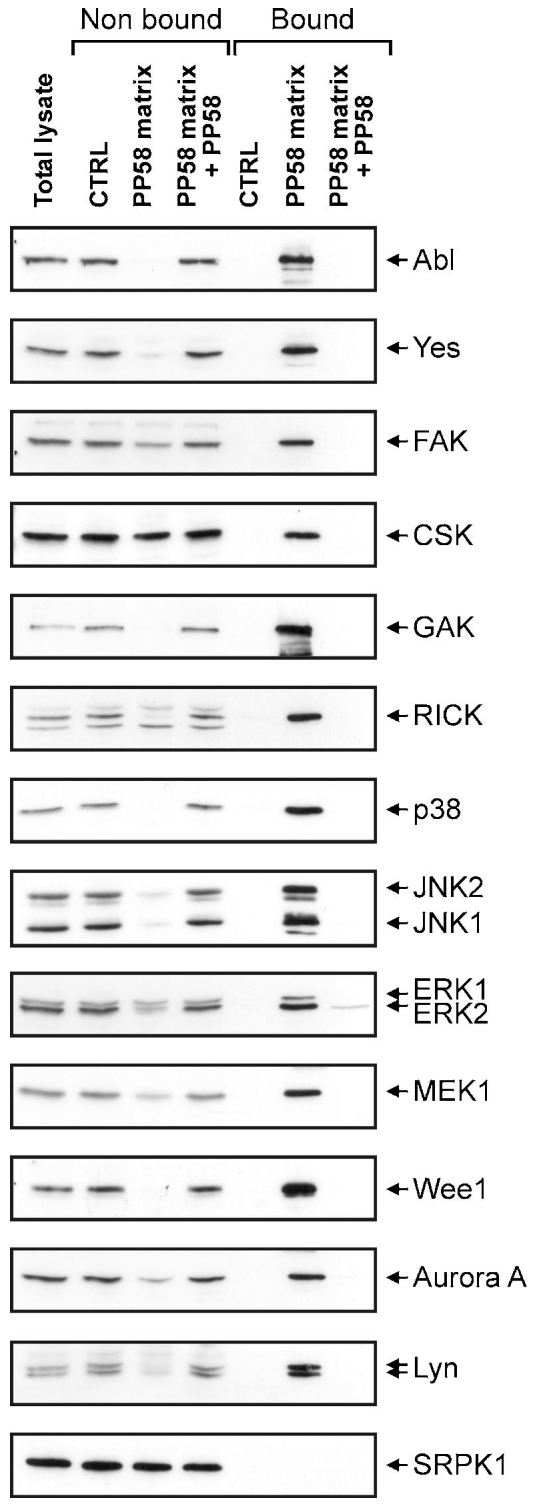

FIG. 4. **Confirmation of MS results by immunoblot analysis.** Total cell lysate from HeLa cells was subjected to *in vitro* association with either control matrix or the PP58 matrix. Free PP58 was added to the incubations where indicated. Total lysate, nonbound proteins from the supernatants and bound proteins eluted from the beads were separated by SDS-PAGE and immunoblotted with specific antibodies against Abl, Yes, FAK, CSK, GAK, RICK, p38, JNK1/2, ERK1/2, MEK1, Wee1, Aurora A, Lyn, and SRPK1.

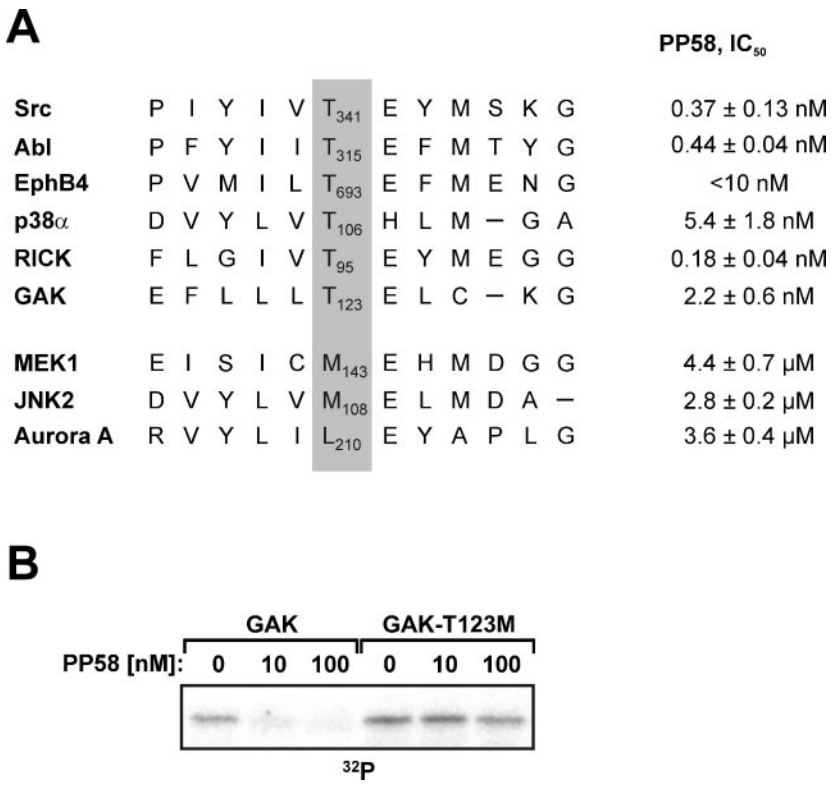

FIG. 5. ***In vitro* assays of cellular protein kinases targeted by the pyrido-[2,3-*d*]pyrimidine inhibitor PP58.** *A*, the activities of several protein kinase targets were measured in the presence of different PP58 concentrations *in vitro* as described under "Experimental Procedures." The determined IC_{50} values for the inhibition of kinase activities by PP58 are shown in comparison to the aligned amino acid sequences surrounding the critical threonine residue at the ATP binding site, which is conserved in most kinase targets with a high affinity for PP58. *B*, recombinant GST-GAK fusion protein possessing the wild-type kinase domain or the corresponding GST-GAK-T123M mutant were assayed for histone phosphorylation *in vitro* at the indicated PP58 concentrations. After SDS-PAGE, substrate protein phosphorylation was detected by autoradiography.

presence of different PP58 concentrations and 50 μM cold ATP. With the exception of the EphB4 receptor tyrosine kinase, we could determine the IC_{50} values of kinase activity inhibition by PP58 for all of the recombinant enzymes tested. In the case of EphB4, the IC_{50} for PP58 inhibition is below 10 nM, but could not be exactly determined due to the relatively low specific activity of the enzyme preparation used. Strikingly, we found that not only tyrosine kinases such as Src and Abl were potently inhibited by PP58 with subnanomolar IC_{50} values, but also identified the Ser/Thr kinases p38α, RICK, and GAK as highly sensitive to inhibition by the pyrido[2,3-*d*]pyrimidine derivative (Fig. 5*A*). RICK showed the lowest IC_{50} value of only 0.18 nM with respect to PP58 inhibition. In stark contrast, 1,000- to 10,000-fold higher PP58 concentrations were required for half maximal inhibition of the Ser/Thr kinases MEK1, JNK2, and Aurora A (Fig. 5*A*). This dramatically lower sensitivity to PP58 correlated with the presence of a larger methionine or leucine side chain at a position where a smaller threonine residue is found in the potently inhibited kinases (Fig. 5*A*). As earlier studies demonstrated for Abl (10, 30) and was recently shown by us for tyrosine kinase targets of pyrido[2,3-*d*]pyrimidine inhibitors such as Src (26), substitution of this critical threonine with a larger amino acid apparently interferes with the extension of the inhibitor's dichlorophenyl moiety into a hydrophobic cavity at the nucleotide-binding pocket and thereby strongly interferes with the binding of the ATP-competitive pyrido[2,3-*d*]pyrimidine inhibitors to these kinase targets. To test whether this structural determinant is also relevant for the highly sensitive Ser/Thr kinases, we mutated the equivalent threonine of GAK to methionine and performed kinase assays with both wild-type and mutant enzyme in the presence of PP58. As shown in Fig. 5*B*, the Thr-123 to methionine mutant of GAK was resistant to PP58 concentrations that completely suppressed the activity of wild-type enzyme. We further quantified the affinity of PP58 for p38α and JNK2 and therefore determined the respective K_i value of PP58 for each kinase. These PP58 targets are closely related kinases but differ in the amino acid residue critical for PP58 sensitivity (Thr-106 in p38α compared with Met-108 in JNK2). The K_i values of PP58 for p38α and JNK2 were 3.8 ± 1.9 nM and 0.32 ± 0.04 μM, respectively, indicating an about 100-fold higher affinity of the inhibitor for p38α than for JNK2. Taken together, our results indicate that the presence of a small residue such as threonine at the relevant site is a structural determinant conserved among high-affinity targets of pyrido[2,3-*d*]pyrimidine inhibitors. However, it is noteworthy that the PP58 affinity matrix also serves as an efficient purification reagent for a variety of protein kinases, which lack this structural feature and have much lower affinities for the pyrido[2,3-*d*]pyrimidine inhibitor PP58.

Cellular Inhibition of p38 and RICK Kinase Activities by the Pyrido[2,3-d]pyrimidine PP58—Pyrido[2,3-*d*]pyrimidine compounds were developed as tyrosine kinase inhibitors for cancer treatment. Our findings that a pyrido[2,3-*d*]pyrimidine derivative effectively targeted the Ser/Thr kinases p38 and RICK, which are both established signal transducers of inflammatory

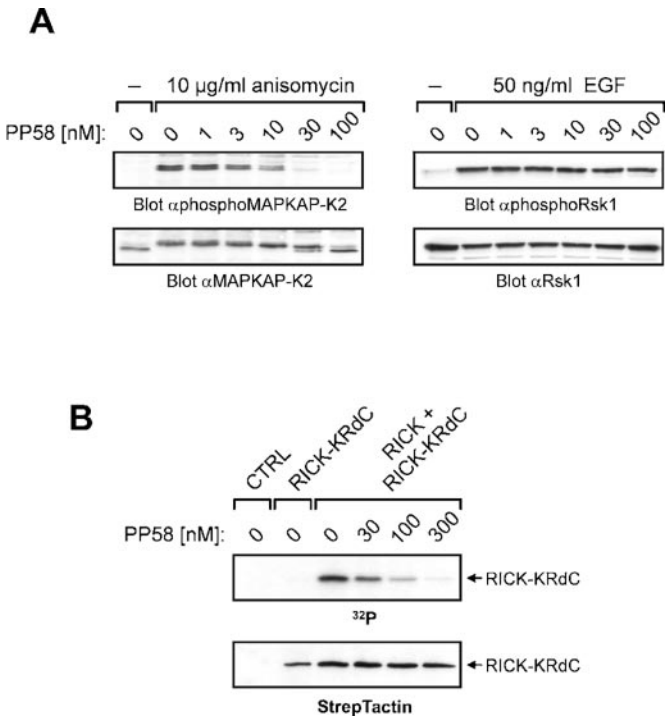

FIG. 6. **Potent inhibition of cellular p38 and RICK kinase activities by the pyrido[2,3-*d*]pyrimidine PP58.** *A*, effect of PP58 on cellular p38 kinase activity. Serum-starved HeLa cells were treated with the indicated PP58 concentrations for 15 min and then either stimulated for 30 min with 10 μg/ml anisomycin or for 5 min with 50 ng/ml EGF prior to cell lysis. Total cell extracts were resolved by gel electrophoresis and then immunoblotted with antisera specifically recognizing phosphorylated Thr-344 in MAPKAP-K2 (*upper left panel*), Rsk1 dually phosphorylated on Thr-359 and Ser-363 (*upper right panel*), MAPKAP-K2 (*lower left panel*), or Rsk1 (*lower right panel*). *B*, cellular inhibition of RICK kinase by PP58. COS-7 cells were transiently transfected with pPM7-RICK-KRdCst expression plasmid (1.35 μg/well) plus either control vector or pPM7-RICK plasmid encoding the full-length kinase (0.15 μg/well). After [^{32}P]orthophosphate labeling and affinity purification using StrepTactin beads, cellular RICK-KRdC phosphorylation was visualized by autoradiography prior to protein detection with StrepTactin-HRP.

responses, prompted us to study the effect of PP58 on their kinase activities in intact cells (35–37). To monitor cellular p38 activity, we analyzed the phosphorylation of its direct cellular substrate MAPKAP-K2 by immunoblotting with phospho-specific antiserum (38). Activation of p38 by anisomycin treatment triggered MAPKAP-K2 phosphorylation at Thr-344, and this stimulation was inhibited by PP58 in a dose-dependent manner with a cellular IC_{50} value somewhat below 10 nM (Fig. 6*A*). Immunoblot analysis with MAPKAP-K2 protein-specific antibody showed the anisomycin-induced band shift of MAPKAP-K2 due to phosphorylation of the protein at multiple sites. This apparent change in molecular weight was also reverted by PP58, albeit at slightly higher concentrations than phosphorylation at Thr-344. In contrast, up to 100 nM PP58 had no effect on the epidermal growth factor (EGF)-stimulated phosphorylation of Rsk1, which is a downstream signaling event mediated through the ERK MAPK cascade. This control experiment illustrates that PP58 can exhibit some degree of selectivity at low nanomolar concentrations *in vivo*.

To investigate the effect of PP58 on RICK activity in intact cells, we performed an assay in which a kinase-inactive RICK fragment serves as a cellular phosphorylation substrate for co-expressed, wild-type enzyme. As shown in Fig. 6*B*, dose-dependent *in vivo* inhibition of RICK activity by PP58 was observed, with as low as 30 nM of the inhibitor already reducing the cellular RICK substrate phosphorylation by more than 50%.

Cellular Inhibition of Cytokine Production by the Pyrido[2,3-d]pyrimidine Compound PP58—Our identification of p38 and RICK as cellular targets of pyrido[2,3-*d*]pyrimidine inhibitors raised the issue whether compounds such as PP58 might suppress inflammatory responses in addition to their cell growth-inhibitory properties. To test this, we first analyzed the effect of PP58 on LPS-induced TNF-α release in primary human PBMCs (39). As seen in Fig. 7*A*, LPS-stimulated TNF-α production was potently inhibited by PP58 with a cellular IC_{50} value of around 3 nM. This effect might be functionally linked to the PP58-mediated suppression of cellular MAPKAP-K2 phosphorylation shown in Fig. 6*A*, because genetic evidence has established this cellular target of p38 kinase as essential transducer of LPS-stimulated TNF-α biosynthesis (40). In addition to TNF-α, we measured the levels of the chemokines MIP-1α and IL-8. LPS-regulated biosynthesis of MIP-1α was also efficiently suppressed by PP58 with an IC_{50} of about 15 nM in human PBMCs, whereas IL-8 production was less susceptible to the pyrido[2,3-*d*]pyrimidine and 100 nM of PP58 reduced the release of this cytokine by about 50%. Compared with PBMCs, the inhibitory effect of 100 nM PP58 on LPS-induced IL-8 production was somewhat more pronounced in human foreskin fibroblasts (Fig. 7*B*). As further shown in Fig. 7*B*, PP58 also interfered with IL-8 biosynthesis upon exposure of cells to the synthetic double-stranded RNA analogue poly(I:C), which acts on toll-like receptor 3 and triggers cellular signaling in a way similar to viral infection (41). The cellular effects of PP58 on cytokine secretion were not a result of general compound toxicity, because up to 100 nM of the inhibitor did not significantly affect cell viability in our assays (data not shown). One of the hallmarks of antiviral responses is the induction of interferons such as IFN-β. Using U373 astrocytoma cells, we investigated the effect of PP58 on poly(I:C)-triggered IFN-β gene induction by quantitative RT-PCR (42). Interestingly, pyrido[2,3-*d*]pyrimidine concentrations as low as 10 nM strongly impaired the synthesis of IFN-β mRNA. Taken together, our results establish the pyrido[2,3-*d*]pyrimidine PP58 as a small molecule antagonist of innate immune responses with potent anti-inflammatory properties.

DISCUSSION

Although inhibitors belonging to the pyrido[2,3-*d*]pyrimidine class of compounds were known to act on several protein kinases, all of these previously described targets belonged to

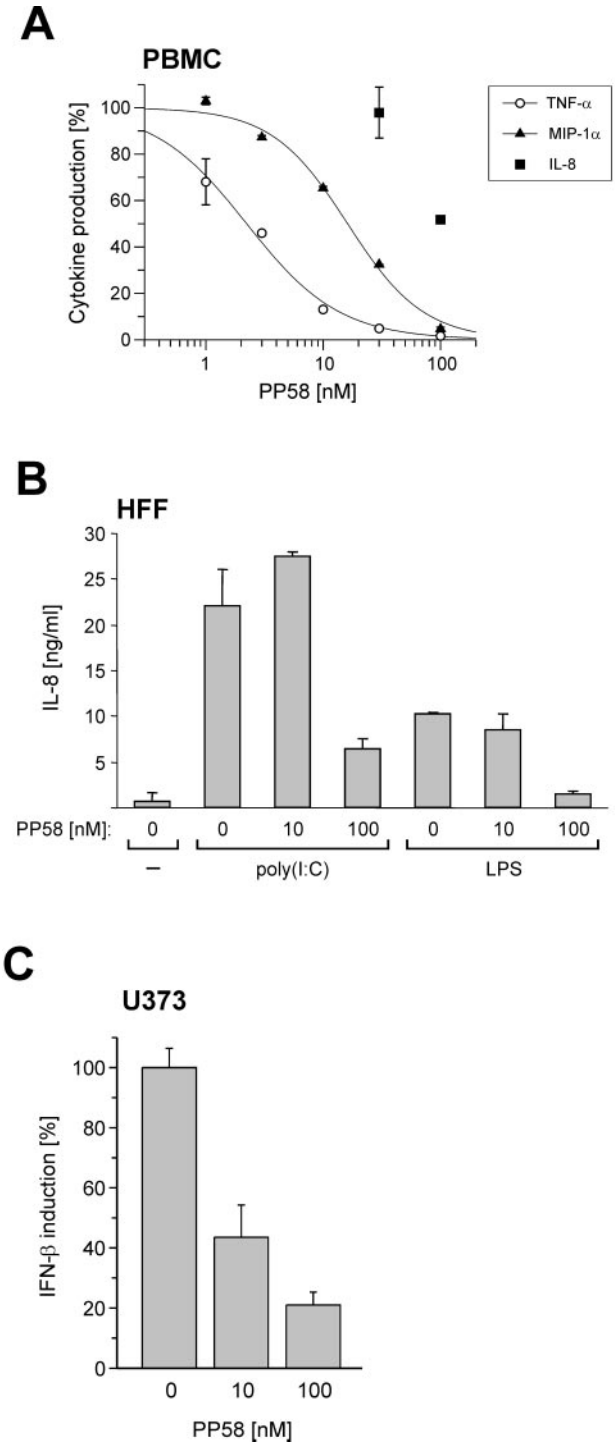

FIG. 7. **Cellular inhibition of LPS- and poly(I:C)-stimulated cytokine induction by the pyrido[2,3-*d*]pyrimidine derivative PP58.** *A*, following 15-min pretreatment with different PP58 concentrations, human PBMCs were stimulated with 1 μg/ml LPS. After 16 h, culture supernatants were harvested and the levels of the released cytokines TNF-α, MIP-1α, and IL-8 were quantified by ELISA. Cytokine levels in the absence of inhibitor were set to 100% and their concentrations in the culture medium in the presence of increasing PP58 doses are expressed relative to this value. The curves of dose-dependent inhibition of TNF-α and MIP-1α production by PP58 were calculated with GraFit. Compared with control-treated monocytes, LPS stimulated the release of TNF-α, MIP-1α, and IL-8 by about 75-, 25-, and 5-fold, respectively. Cytokine levels in the supernatant from LPS-treated cells were 12 ng/ml (TNF-α), 70 ng/ml (MIP-1α), and 247 ng/ml (IL-8). *B*, HFF cells were pretreated with Me_2SO or the indicated PP58 concentrations for 15 min and then stimulated with either 50 μg/ml poly(I:C) or 1 μg/ml LPS. After 16 h, IL-8 levels in the cell culture supernatants were measured by ELISA. *C*, following preincubation with the indicated PP58 concentrations for 15 min, U373 astrocytoma cells were stimulated for 2 h with 50 μg/ml poly(I:C) prior to lysis and RNA isolation. After reverse transcription, quantitative PCR was performed to measure IFN-β gene induction in control incubated and poly(I:C)-treated cells. Transcript levels in IFN-β-treated cells were set to 100% and the levels upon inhibitor treatment are shown relative to this value.

the tyrosine kinase family and it therefore appeared that pyrido[2,3-*d*]pyrimidine inhibitors are selective for this particular group of the human kinome (6–9). The results presented here identify several Ser/Thr kinases as highly sensitive pyrido[2,3-*d*]pyrimidine targets, and, moreover, these protein kinases belong to different groups of the human kinome. Thus, sensitivity to pyrido[2,3-*d*]pyrimidine inhibition does not closely correlate with phylogenetic relationship (17). Instead, a small residue at the ATP binding pocket, usually a threonine, is conserved in all of the highly sensitive kinases. This structural determinant permits the projection of the dichlorophenyl substituent of the inhibitor into a hydrophobic pocket adjacent to the ATP binding site. At the ATP binding site itself, other parts of the inhibitor such as its pyrido[2,3-*d*]pyrimidine core structure are bound to the same region as the adenine moiety of ATP (26). Importantly, the hydrophobic pocket does not interact with any part of a kinase-bound ATP molecule, explaining why the substitution of the critical threonine with a larger residue such as methionine sterically interferes with inhibitor binding, but does not abrogate protein kinase activity. The relevance of this structural motif was previously documented for tyrosine kinases and also applies to Ser/Thr kinases, as shown for GAK by mutational analysis (10, 26). However, our affinity method also resulted in the efficient purification of several targets, mostly Ser/Thr kinases, which had a large hydrophobic residue such as methionine at the critical position. Consistent with the sterical clash conferred by such a bulky side chain, these kinases were inhibited by the pyrido[2,3-*d*]pyrimidine PP58 with micromolar IC_{50} values and not with the low nanomolar or even subnanomolar IC_{50} values determined for kinases such as p38, RICK, and GAK. These secondary assays in combination with K_i determinations for p38α and JNK2 confirmed that the pyrido[2,3-*d*]pyrimidine inhibitor beads permitted the enrichment of protein kinases with dramatically different relative affinities to the inhibitor. The efficient purification of target kinases that are only affected in the presence of micromolar inhibitor concentrations *in vitro* further indicates that the covalent linkage of PP58 to the matrix did not result in steric hindrance with respect to kinase binding, and this conclusion is consistent

with the data from Src kinase assays obtained with the pegylated inhibitor derivative. To our knowledge, the pyrido[2,3-*d*]pyrimidine inhibitor matrix allowed the purification and identification of more human protein kinases than found in any previous proteomic study. Thus, the PP58 resin provides a useful reagent to compare kinase expression levels of a significant subset of the kinome. Potential applications of this new biochemical tool involve expression analysis of potential drug targets in different human tumor cells. Such an experimental approach could lead to important findings, as relevant oncogenic protein kinases are frequently present at elevated levels in human cancer (43, 44).

A significant outcome of the present study is the identification of p38 and RICK as pyrido[2,3-*d*]pyrimidine inhibitor targets in the context of the potent anti-inflammatory effects observed for the derivative PP58, for the following reasons: The pyrido[2,3-*d*]pyrimidine PD166285 was reported to have good oral bioavailability in rats by Klutschko *et al.* (8). Strikingly, PD166285 was converted via an intermediate into a final metabolite, which then was detected at stable plasma concentrations of more than 100 nM over at least 24 h. This stable metabolite was the PP58 derivative used in this study. Given the potent inhibition of LPS-induced TNF-α biosynthesis observed in primary monocytes at much lower PP58 concentrations *in vitro*, an obvious speculation is that similar anti-inflammatory effects should be seen in animals upon oral application of pyrido[2,3-*d*]pyrimidines such as PD166285. This remains to be tested. In a sense, positive results from such an animal study would validate our chemical proteomic approach as a valuable tool to link previously unrecognized therapeutic areas to existing drugs.

A major concern with the use of pyrido[2,3-*d*]pyrimidines such as PD166285 or the PP58 derivative is their apparent lack of specificity. However, there are data from earlier medicinal chemistry studies demonstrating that the selectivity of pyrido[2,3-*d*]pyrimidine-based compounds can be improved. For example, a 3,5-dimethoxyphenyl instead of the 2,6-dichlorophenyl functionality present in the 6-position was shown to dramatically increase the selectivity of pyrido[2,3-*d*]pyrimidines for the FGFR (45, 46). These derivatives were then inactive against other targets such as Src. Thus, there seems to be potential for optimizing this potent compound class for other targets such as p38 kinase, which could ultimately result into the development of novel drugs for the treatment of human disease.

Acknowledgments—We thank Robert Brehm and Kirsten Minkhart for excellent technical assistance. We also would like to thank Dirk Wehmhöner and Manfred Nimtz for providing access to a Q-TOF II instrument.

* This work was supported by a grant from the German Bundesministerium für Bildung und Forschung. The costs of publication of this article were defrayed in part by the payment of page charges. This article must therefore be hereby marked "*advertisement*" in accordance with 18 U.S.C. Section 1734 solely to indicate this fact.

‡ To whom correspondence should be addressed: Axxima Pharmaceuticals AG, Max-Lebsche-Platz 32, 81377 München, Germany. Tel.: 49-89-550-65-356; Fax: 49-89-550-65-461; E-mail: henrik.daub@axxima.com.

REFERENCES

1. Cohen, P. (2002) Protein kinases—the major drug targets of the twenty-first century? *Nat. Rev. Drug Discov.* **1,** 309–315
2. Capdeville, R., Buchdunger, E., Zimmermann, J., and Matter, A. (2002) Glivec (STI571, imatinib), a rationally developed, targeted anticancer drug. *Nat. Rev. Drug Discov.* **1,** 493–502
3. Gorre, M. E., Mohammed, M., Ellwood, K., Hsu, N., Paquette, R., Rao, P. N., and Sawyers, C. L. (2001) Clinical resistance to STI-571 cancer therapy caused by BCR-ABL gene mutation or amplification. *Science* **293,** 876–880
4. Shah, N. P., Nicoll, J. M., Nagar, B., Gorre, M. E., Pacquette, R. L., Kuriyan, J., and Sawyers, C. L. (2002) Multiple *BCR-ABL* kinase domain mutations confer polyclonal resistance to the tyrosine kinase inhibitor imatinib (STI571) in chronic phase and blast crisis chronic myeloid leukemia. *Cancer Cell* **2,** 117–125
5. von Bubnoff, N., Schneller, F., Peschel, C., and Duyster J. (2002) *BCR-ABL* gene mutations in relation to clinical resistance of Philadelphia-chromosome-positive leukaemia to STI571: A prospective study. *Lancet* **359,** 487–491
6. Dorsey, J. F., Jove, R., Kraker, A. J., and Wu, J. (2000) The pyrido[2,3-*d*]-pyrimidine derivative PD180970 inhibits p210Bcr-Abl tyrosine kinase and induces apoptosis of K562 leukemic cells. *Cancer Res.* **60,** 3127–3131
7. Panek, R. L., Lu, G. H., Klutschko, S. R., Batley, B. L., Dahring, T. K., Hamby, J. M., Hallak, H., Doherty, A. M., and Keiser, J. A. (1997) *In vitro* pharmacological characterization of PD 166285, a new nanomolar potent and broadly active protein tyrosine kinase inhibitor. *J. Pharmacol. Exp. Ther.* **283,** 1433–1444
8. Klutschko, S. R., Hamby, J. M., Boschelli, D. H., Wu, Z., Kraker, A. J., Amar, A. M., Hartl, B. G., Shen, C., Klohs, W. D., Steinkampf, R. W., Driscoll, D. L., Nelson, J. M., Elliott, W. L., Roberts, B. J., Stoner, C. L., Vincent, P. W., Dykes, D. J., Panek, R. L., Lu, G. H., Major, T. C., Dahring, T. K., Hallak, H., Bradford, L., Showalter, H. D. H., and Doherty, A. M. (1998) 2-Substituted aminopyrido[2,3-*d*]pyrimidin-7(8H)-ones. Structure-activity relationships against selected tyrosine kinases and *in vitro* and *in vivo* anticancer activity. *J. Med. Chem.* **41,** 3276–3292
9. Wisniewski, D., Lambek, C. L., Liu, C., Strife, A., Veach, D., R., Nagar, B., Young, M. A., Schindler, T., Bornmann, W. G., Bertino, J. R., Kuriyan, J., and Clarkson, B. (2002) Characterization of potent inhibitors of the Bcr-Abl and the c-kit receptor tyrosine kinases. *Cancer Res.* **62,** 4244–4255
10. La Rosée, P., Corbin, A. S., Stoffregen, E. P., Deininger, M. W., and Druker, B. J. (2002) Activity of the Bcr-Abl kinase inhibitor PD180970 against clinically relevant Bcr-Abl isoforms that cause resistance to imatinib mesylate (Gleevec, STI571). *Cancer Res.* **62,** 7149–7153
11. Branford, S., Rudzki, Z., Walsh, S., Grigg, A., Arthur, C., Taylor, K., Herrmann, R., Lynch, K. P., and Hughes, T. P. (2002) High frequency of point mutations clustered within the adenosine triphosphate-binding region of BCR/ABL in patients with chronic myeloid leukemia or Ph-positive acute lymphoblastic leukemia who develop imatinib (STI571) resistance. *Blood* **99,** 3472–3475
12. Hofmann, W.-K., Jones, L. C., Lemp, N. A., de Vos, S., Gschaidmeier, H., Hoelzer, D., Ottmann, O. G., and Koeffler, H. P. (2002) Ph(+) acute lymphoblastic leukemia resistant to the tyrosine kinase inhibitor STI571 has a unique BCR-ABL gene mutation. *Blood* **99,** 1860–1862
13. Dimitroff, C. J., Klohs, W., Sharma, A., Pera, P., Driscol, l D., Veith, J., Steinkampf, R., Schroeder, M., Klutchko, S., Sumlin, A., Henderson, B., Dougherty, T. J., and Bernacki, R. J. (1999) Anti-angiogenic activity of selected receptor tyrosine kinase inhibitors, PD166285 and PD173074: implications for combination treatment with photodynamic therapy. *Invest. New Drugs* **17,** 121–135
14. Kraker, A. J., Roberts, B. J., Vincent, P. W., Patmore, S. J., and Elliott, W. (1999) *In vivo* antitumor activity of selective c-src tyrosine kinase (TK) inhibitors. *Proc. Am. Assoc. Cancer Res.* **40,** 808
15. Davies, S. P., Reddy, H., Caivano, M., and Cohen, P. (2000) Specificity and mechanism of action of some commonly used protein kinase inhibitors. *Biochem. J.* **351,** 95–105

16. Bain, J., McLauchlan, H., Elliott, M., and Cohen, P. (2003) The specificities of protein kinase inhibitors: An update. *Biochem. J.* **371,** 199–204
17. Manning, G., Whyte, D. B., Martinez, R., Hunter, T., and Sudarsanam, S. (2002) The protein kinase complement of the human genome. *Science* **298,** 1912–1934
18. Knockaert, M., Gray, N., Damiens, E., Chang, Y.-T., Grellier, P., Grant, K., Fergusson, D., Mottram, J., Soete, M., Dubremetz, K.-F., Le Roch, K., Doerig, C., Schultz, P. G., and Meijer, L. (2000) Intracellular targets of cyclin-dependent kinase inhibitors: Identification by affinity chromatography using immobilised inhibitors. *Chem. Biol.* **7,** 411–422
19. Knockaert, M., Wieking, K., Schmitt, S., Leost, M., Grant, K. M., Mottram, J. C., Kunick, C., and Meijer, L. (2002) Intracellular targets of paullones. Identification following affinity purification on immobilized inhibitor. *J. Biol. Chem.* **277,** 25493–25501
20. Brown, D., and Superti-Furga, G. (2003) Rediscovering the sweet spot in drug discovery. *Drug Discov. Today* **8,** 1067–1077
21. Wan, Y., Hur, W., Cho, C. Y., Liu, Y., Adrian, F. J., Lozach, O., Bach, S., Mayer, T., Fabbro, D., Meijer, L., and Gray, N. S. (2004) Synthesis and target identification of hymenialdisine analogs. *Chem. Biol.* **11,** 247–259
22. Godl, K., Wissing, J., Kurtenbach, A., Habenberger, P., Blencke, S., Gutbrod, H., Salassidis, K., Stein-Gerlach, M., Missio, A., Cotten, M., and Daub, H. (2003) An efficient proteomics method to identify the cellular targets of protein kinase inhibitors. *Proc. Natl. Acad. Sci. U. S. A.* **100,** 15434–15439
23. Brehmer, D., Godl, K., Zech, B., Wissing, J., and Daub, H. (2004) Proteome-wide identification of cellular targets affected by bisindolylmaleimide-type protein kinase C inhibitors. *Mol. Cell. Proteomics* **3,** 490–500
24. Godl, K., and Daub, H. (2004) Proteomic analysis of kinase inhibitor selectivity and function. *Cell Cycle* **3,** 393–395
25. Cotten, M., Stegmueller, K., Eickhoff, J., Herzberger, K., Herget, T., Choidas, A., Daub, H., and Godl, K. (2003) Exploiting features of adenovirus replication to support mammalian kinase production. *Nucleic Acids Res.* **31,** e128
26. Blencke, S., Zech, B., Engkvist, O., Greff, Z., Orfi, L., Horvath, Z., Keri, G., Ullrich, A., and Daub, H. (2004) Characterization of a conserved structural determinant controlling protein kinase sensitivity to selective inhibitors. *Chem. Biol.* **11,** 691–701
27. Daub, H., Blencke, S., Habenberger, P., Kurtenbach, A., Dennenmoser, J., Wissing, J., Ullrich, A., and Cotten, M. (2002) Identification of SRPK1 and SRPK2 as the major cellular protein kinases phosphorylating hepatitis B virus core protein. *J. Virol.* **76,** 8124–8137
28. Beardsley, R. L., and Reilly, J. P. (2002) Optimization of guanidination procedures for MALDI mass mapping. *Anal. Chem.* **74,** 1884–1890
29. Wang, Y., Li, R., Booher, R. N., Kraker, A., Lawrence, T., Leopold, W. R., and Sun, Y. (2001) Radiosensitization of p53 mutant cells by PD0166285, a novel G(2) checkpoint abrogator. *Cancer Res.* **61,** 8211–8217
30. Nagar, B., Bornmann, W. G., Pellicena, P., Schindler, T., Veach, D. R., Miller, W. T., Clarkson, B., and Kuriyan, J. (2002) Crystal structures of the kinase domain of c-Abl in complex with the small molecule inhibitors PD173955 and imatinib (STI-571). *Cancer Res.* **62,** 4236–4243
31. Wang, Q., Smith, J. B., Harrison, M. L., and Geahlen, R. L. (1991) Identification of tyrosine 67 in bovine brain myelin basic protein as a specific phosphorylation site for thymus p56lck. *Biochem. Biophys. Res. Commun.* **178,** 1393–1399
32. Superti-Furga, G., Fumagalli, S., Kögl, M., Courtneidge, S. A., and Draetta, G. (1993) Csk inhibition of c-Src activity requires both the SH2 and SH3 domains of Src. *EMBO J.* **12,** 2625–2634
33. Schmidt, F., Donahoe, S., Hagens, K., Mattow, J., Schaible, U. E., Kaufmann, S. H., Aebersold, R., and Jungblut, P. R. (2004) Complementary analysis of the Mycobacterium tuberculosis proteome by two-dimensional electrophoresis and isotope-coded affinity tag technology. *Mol. Cell. Proteomics* **3,** 24–42
34. Wang, J., Xue, Y., Feng, X., Li, X., Wang, H., Li, W., Zhao, C., Cheng, X., Ma, Y., Zhou, P., Yin, J., Bhatnagar, A., Wang, R., and Liu, S. (2004) An analysis of the proteomic profile for *Thermoanaerobacter tengcongensis* under optimal culture conditions. *Proteomics* **4,** 136–150
35. Lee, J. C., Laydon, J. T., McDonell, P. C., Gallagher, T. F., Kumar, S., Green, D., McNulty, D., Blumenthal, M. J., Heys, J. R., Landvatter, S. W., Strickler, J. E., McLaughlin, M. M., Siemens, I. R., Fisher, S. M., Livi, G. P., White, J. R., Adams, J. L., and Young, P. R. (1994) A protein kinase involved in the regulation of inflammatory cytokine biosynthesis. *Nature* **372,** 739–746
36. Chin, A. I., Dempsey, P. W., Bruhn, K., Miller, J. F., and Cheng, G. (2002) Involvement of receptor-interacting protein 2 in innate and adaptive immune responses. *Nature* **416,** 190–194
37. Kobayashi, K., Inohara, N., Hernandez, L. D., Galan, J. E., Nunez, G., Janeway, C. A., Medzhitov, R., and Flavell, R. A. (2002) RICK/Rip2/CARDIAK mediates signalling for receptors of the innate and adaptive immune systems. *Nature* **416,** 194–199
38. Eyers, P. A., van den Ijssel, P., Quinlan, R. A., Goedert, M., and Cohen, P. (1999) Use of a drug-resistant mutant of stress-activated protein kinase 2a/p38 to validate the in vivo specificity of SB 203580. *FEBS Lett.* **451,** 191–196
39. Rutault, K., Hazzalin, C. A., and Mahadevan, L. C. (2001) Combinations of ERK and p38 MAPK inhibitors ablate tumor necrosis factor-α (TNF-α) mRNA induction. Evidence for selective destabilization of TNF-α transcripts. *J. Biol. Chem.* **276,** 6666–6674
40. Kotlyarov, A., Neininger, A., Schubert, C., Eckert, R., Birchmeier, C., Volk, H.-D., and Gaestel, M. (1999) MAPKAP kinase 2 is essential for LPS-induced TNF-α biosynthesis. *Nat. Cell Biol.* **1,** 94–97
41. Akira, S. (2003) Mammalian Toll-like receptors. *Curr. Opin. Immunol.* **15,** 5–11
42. Servant, M. J., Grandvaux, N., tenOever, B. R., Duguay, D., Lin, R., and Hiscott, J. (2003) Identification of the minimal phosphoacceptor site required for *in vivo* activation of interferon regulatory factor 3 in response to virus and double-stranded RNA. *J. Biol. Chem.* **278,** 9441–9447
43. Dancey, J., and Sausville, E.A. (2003) Issues and progress with protein kinase inhibitors for cancer treatment. *Nat. Rev. Drug Discov.* **2,** 296–313
44. Fischer, O. M., Streit, S., Hart, S., and Ullrich, A. (2003) Beyond Herceptin and Gleevec. *Curr. Opin. Chem. Biol.* **7,** 490–495
45. Hamby, J. M., Connolly, C. J., Schroeder, M. C., Winters, R. T., Showalter, H. D., Panek, R. L., Major, T. C., Olsewski, B., Ryan, M. J., Dahring, T., Lu, G. H., Keiser, J., Amar, A., Shen, C., Kraker, A. J., Slintak, V., Nelson, J. M., Fry, D. W., Bradford, L., Hallak, H., and Doherty, A. M. (1997) Structure-activity relationships for a novel series of pyrido[2,3-*d*]pyrimidine tyrosine kinase inhibitors. *J. Med. Chem.* **40,** 2296–2303
46. Mohammadi, M., Froum, S., Hamby, J. M., Schroeder, M. C., Panek, R. L., Lu, G. H., Eliseenkova, A. V., Green, D., Schlessinger, J., and Hubbard, S. R. (1998) Crystal structure of an angiogenesis inhibitor bound to the FGF receptor tyrosine kinase domain. *EMBO J.* **17,** 5896–5904